Review

Structural advances for the major facilitator superfamily (MFS) transporters

Nieng Yan

State Key Laboratory of Bio-membrane and Membrane Biotechnology, Center for Structural Biology, School of Medicine, Tsinghua-Peking Center for Life Sciences, Tsinghua University, Beijing 100084, China

The major facilitator superfamily (MFS) is one of the largest groups of secondary active transporters conserved from bacteria to humans. MFS proteins selectively transport a wide spectrum of substrates across biomembranes and play a pivotal role in multiple physiological processes. Despite intense investigation, only seven MFS proteins from six subfamilies have been structurally elucidated. These structures were captured in distinct states during a transport cycle involving alternating access to binding sites from either side of the membrane. This review discusses recent progress in MFS structure analysis and focuses on the molecular basis for substrate binding, co-transport coupling, and alternating access.

The major facilitator superfamily

Transmembrane movement of solutes is vital for the growth and homeostasis of all cells. A limited number of small molecules can freely diffuse across the lipid bilayer and bulk translocation can be achieved through endocytosis and exocytosis. However, selective transport of most solutes and specific substrates across the lipid bilayer is mediated by a great variety of transport proteins, including transporters and channels, which are present in every single cell. Among these, the MFS [Transporter Classification Database (TCDB) #2.A.1] is an ancient and ubiquitous transporter family found in all kingdoms of life [1–3]. The MFS contains more than 10 000 sequenced members, representing the largest family of secondary transporters. The number of MFS proteins identified continues to rise with the rapidly growing number of genomes sequenced [Saier, M.H. and Reddy, V. (2012) Transporter Classification Database (http://www.tcdb.org/)].

MFS transporters target a wide spectrum of substrates including ions, carbohydrates, lipids, amino acids and peptides, nucleosides, and other molecules. On the basis of phylogenetic analysis, substrate specificity, and working mechanism, the MFS is divided into 76 subfamilies in the TCDB [Saier, M.H. and Reddy, V. (2012) Transporter Classification Database (http://www.tcdb.org/)]. Nearly half of the MFS subfamilies are of unknown or only putative functions, whereas a few others, exemplified by the *Escherichia coli* lactose permease LacY, have been rigorously characterized. LacY is a prototypical secondary active transporter that has been studied for almost half a century using molecular, genetic, biochemical, and biophysical approaches [4,5]. It now represents a model system for the development and validation of new technologies [6,7].

MFS transporters function in a multitude of physiological processes. For instance, members of the sugar porter (SP) subfamily (TCDB #2.A.1.1) are vital for metabolism and energy homeostasis in bacteria, archaea, fungi, protozoa, plants, and animals because they mediate the cellular uptake of glucose and other mono- and disaccharides [8–13]. The DHA1 and DHA2 subfamilies (drug:H^+ antiporters 1/2, TCDB #2.A.1.2/3) play a major role in multidrug resistance in bacteria and fungi [14–19]. In humans, the rigorously studied glucose transporters GLUT1, 2, 3, and 4 are responsible for glucose uptake into organs and tissues.

Changes in function, expression, or localization of MFS transporters are associated with various human diseases. For instance, missense mutations of GLUT1 may lead to GLUT1 deficiency syndrome (also known as De Vivo disease) characterized by infantile-onset seizures, delayed growth, and mental retardation [20,21]. Mutations of GLUT2 are associated with the Fanconi–Bickel syndrome [22]. By contrast, the expression levels of GLUT1 and GLUT3 are enhanced in certain cancer cell lines to support the increased demand for glucose in tumor cells (the Warburg effect) [23,24]. The localization of GLUT4, the major glucose transporter in skeletal muscles and adipocytes, is subject to insulin regulation through a complex signaling mechanism; dysfunction of this mechanism is implicated in obesity and type 2 diabetes mellitus [25–27].

General structural features of MFS proteins

Because of their physiological significance, MFS proteins have been popular targets for structural and mechanistic investigations, with the potential to provide important information both for elucidating membrane protein biology and for understanding diseases. Despite the large number of sequenced MFS members, progress in their structural studies has remained relatively slow since the reports of the first two MFS structures a decade ago [28,29]. At present, crystal structures have been reported for only seven MFS proteins comprising six distinct MFS subfamilies (Table 1; Membrane proteins of known 3D structure,

Corresponding author: Yan, N. (nyan@tsinghua.edu.cn).
Keywords: major facilitator superfamily; 3-TM (transmembrane segments) repeat; alternating access; structure.

Table 1. MFS proteins of known structure

Protein	Function	MFS subfamily	TCDB number	Organism	PDB code	Resolution limit (Å)	Year of publication
LacY	Lactose:proton symporter	Oligosaccaride:H^+ symporter (OHS)	2.A.1.5.1	*Escherichia coli*	1PV6, 1PV7, 2CFP, 2CFQ, 2V8N, 2Y5Y	2.95	2003
GlpT	Glycerol-3-phosphate: Pi antiporter	Organophosphate: Pi antiporter (OPA)	2.A.1.4.3	*Escherichia coli*	1P24	3.3	2003
EmrD	Multidrug transproter	Drug:H^+ antiporter-1 (DHA1)	2.A.1.2.9	*Escherichia coli*	2GFP	3.5	2006
FucP	L-Fucose:proton symporter	Fucose:H^+ symporter (FHS)	2.A.1.7.1	*Escherichia coli*	3O7Q, 3O7P	3.1	2009
$PepT_{so}$	Peptide:proton symporter	Proton-dependent Oligopeptide Transporter (POT)	2.A.17	*Shewanella oneidensis*	2XUT	3.6	2011
$PepT_{st}$	Peptide:proton symporter	POT		*Streptococcus thermophilus*	4APS	3.3	2012
XylE	D-Xylose:proton symporter	Sugar porter (SP)	2.A.1.1.3	*Escherichia coli*	4GBY, 4GBZ, 4GC0	2.6	2012

http://blanco.biomol.uci.edu/mpstruc/listAll/list). In chronological order of their publication, these are structures of the lactose:H^+ symporter LacY [28], the glycerol-3-phosphate:Pi antiporter GlpT [29], the multidrug:H^+ antiporter EmrD [30], the L-fucose:H^+ symporter FucP [31], the oligopeptide:H^+ symporters $PepT_{so}$ from *Shewanella oneidensis* [32] and $PepT_{st}$ from *Streptococcus thermophilus* [33], and the D-xylose:H^+ symporter XylE [34] (Figure 1 and Table 1).

Bioinformatic analysis predicted that the majority of MFS members comprise 12 transmembrane helices (TMs), with some containing more [3,35,36]. Both the N and C termini of an MFS are usually located on the cytoplasmic side of the membrane. Although proteins from the six subfamilies exhibit low sequence similarity, distinct substrate specificities, and different transport coupling mechanisms, they all share a common structural fold, known as

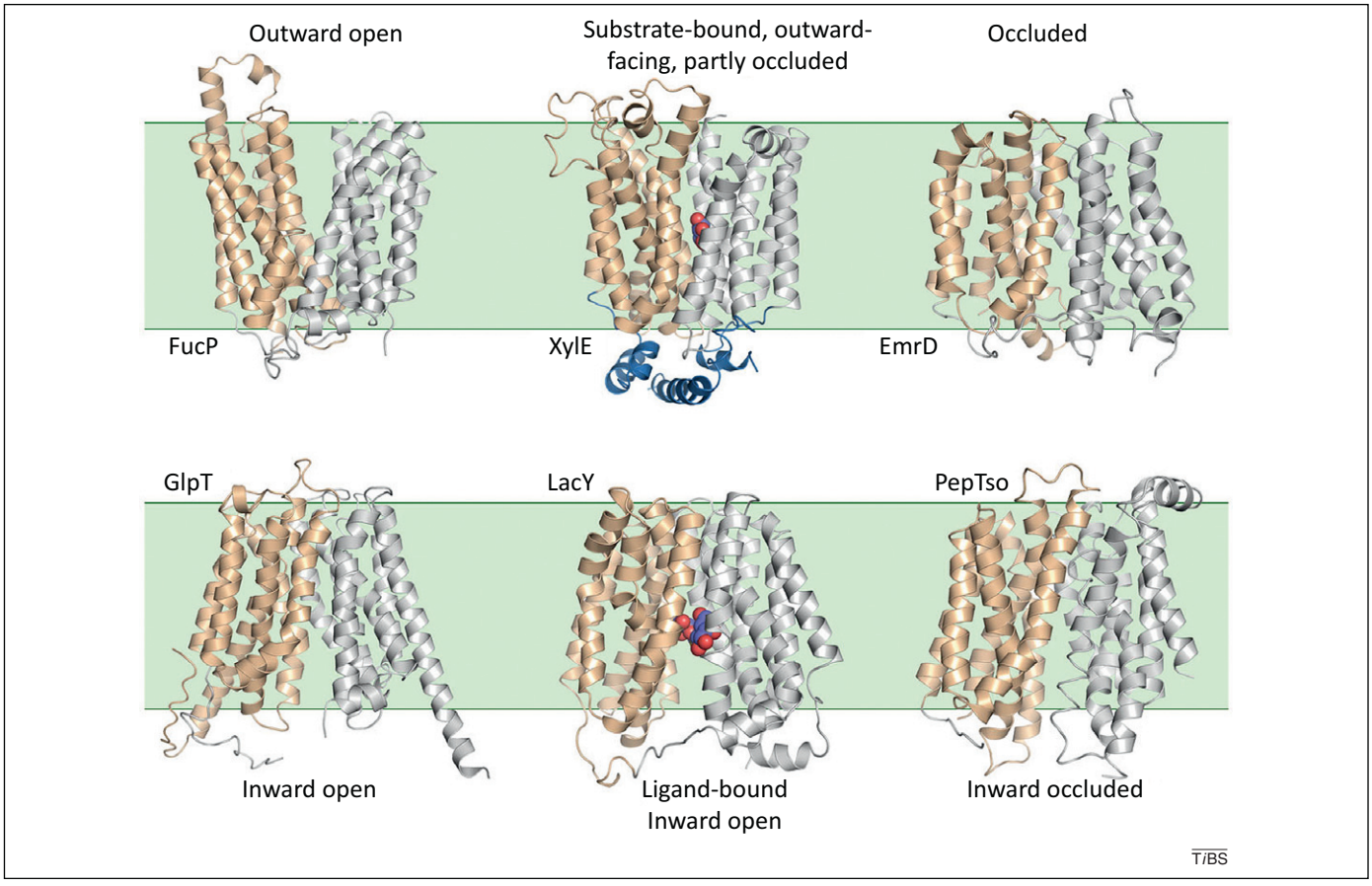

Figure 1. Distinct conformational states of major facilitator superfamily (MFS) transporters. The available structures of MFS transporters, except that of $PepT_{st}$, are shown. The distinct N and C domains are colored wheat and silver, respectively. The intracellular helix domain unique to XylE is colored blue. The bound ligands in XylE and LacY are shown as spheres. Conformational states of these MFS members during a transport cycle are indicated above (top row) or below (bottom row) the structures. The PDB accession codes for these structures are 3O7Q for FucP, 4GBY for XylE, 2GFP for EmrD, 2XUT for $PepT_{so}$, 1PV7 for LacY, and 1PW4 for GlpT. An inventory of these structures is shown in Table 1. All structure figures were prepared using PyMol (http://www.pymol.org). In all side views throughout the manuscript, the transporters are positioned with the periplasmic side on the top and the cytoplasmic side on the bottom.

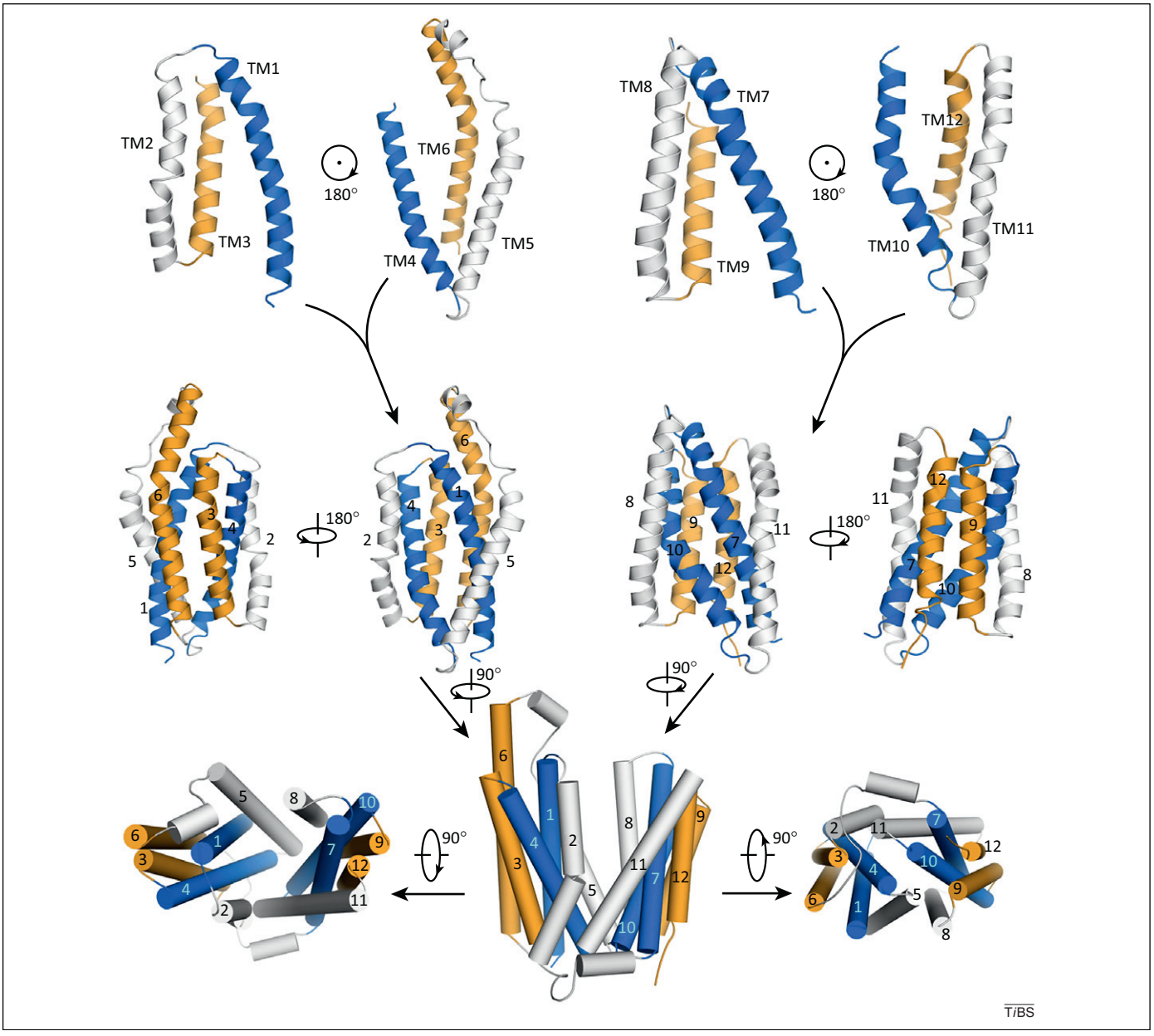

Figure 2. A canonical major facilitator superfamily (MFS) fold. A canonical 12-TM (transmembrane segment) MFS fold contains four 3-TM repeats (top row). Two inverted 3-TM repeats constitute one distinct domain (middle row). The two domains in an MFS fold are related by an approximate 180° rotation around an axis that is perpendicular to the plane of the lipid membrane (bottom row). The corresponding TMs in each 3-TM unit are colored the same. The same color scheme is used in Figures 3 and 5.

the MFS fold (Figure 2). A canonical MFS fold comprises 12 TMs that are organized into two discretely folded domains, the N and C domains, each containing six consecutive TMs. The N and C domains, despite little sequence similarity, display a twofold pseudosymmetry related by an axis perpendicular to the membrane plane.

Primary sequence analyses of several MFS proteins have suggested a duplicated 3-TM [37], or a triplicated 2-TM repeat based on other criteria [3]. Structural and functional analyses favor the division of each domain into a pair of inverted 3+3 repeats (Figure 2). TMs 1/2/3 and TMs 4/5/6 in the N domain are related by an approximate 180° rotation around an axis that runs parallel to the membrane bilayer; so are TMs 7/8/9 and TMs 10/11/12 in the C domain (Figure 2) [29,31,38]. In LacY, the 3-TM repeats in the N and C domains can be superimposed with root-mean-square deviation (RMSD) values of 3.8 and 3.3 Å, respectively [38]. In FucP, the four sets of 3-TM repeats can be superposed with a pairwise RMSD ranging between 2.1 and 3.4 Å over approximately 80 Cα atoms. Such intrastructural comparisons support the notion that the 3-TM repeat represents a fundamental structural unit for MFS proteins.

The corresponding TMs in each 3-TM repeat appear to play similar structural and functional roles [28–34]. In all MFS structures, TMs 1, 4, 7, and 10 are positioned in the center of the transporter, contributing the majority of the residues essential for substrate coordination and co-transport coupling. These TMs are also involved in the interactions between N and C domains of the transporter. TMs 2, 5, 8, and 11 are positioned on the sides of the structure and mediate the bulk of the interdomain contacts. Residues

from these TMs may also participate in substrate binding and co-transport coupling [39]. TMs 3, 6, 9, and 12 are placed on the outside of TMs 1, 4, 7, and 10 and are important for structural integrity (Figure 2, bottom row). Therefore, the 3-TM repeat appears to be the basic functional unit for an MFS fold. Interestingly, in terms of overall structural organization, corresponding TMs from two 3-TM repeats are always positioned next to each other in opposite transmembrane orientations (Figure 2).

It is noteworthy that the connecting segments, particularly the cytoplasmic ones, between consecutive TMs may play an important role [34]. Despite the low sequence similarity among MFS proteins, two conserved sequences, DRXXRR, are found at the tightly joined cytoplasmic ends of TMs 2 and 3 and of TMs 8 and 9 in the N and C domains, respectively, in a large number of MFS members [40]. As seen in the seven MFS structures, the two cytoplasmic loops between TMs 2 and 3 and TMs 8 and 9 are all short, a structural feature that provides restraint to the relative motions of the connected TMs on the cytoplasmic side. By contrast, the linker that connects the two domains of an MFS fold is usually long, consisting of 30 to nearly 100 residues, and exists in the form of unstructured loop [28–33] or α-helices [34]. Such structural features may support a large degree of relative motion between the two domains during an alternating access cycle of an MFS transporter [31].

Alternating access

The working mechanism of all membrane transporters may be represented by a general alternating access model, in which the substrate binding site(s) is alternately exposed to either side of the membrane [41]. To complete a transport cycle, a transporter must undergo distinct conformational shifts, producing the outward-facing, occluded, and inward-facing states for upload and release of substrate(s) across the lipid bilayer (Figure 3a). During this process, the bound substrate(s)

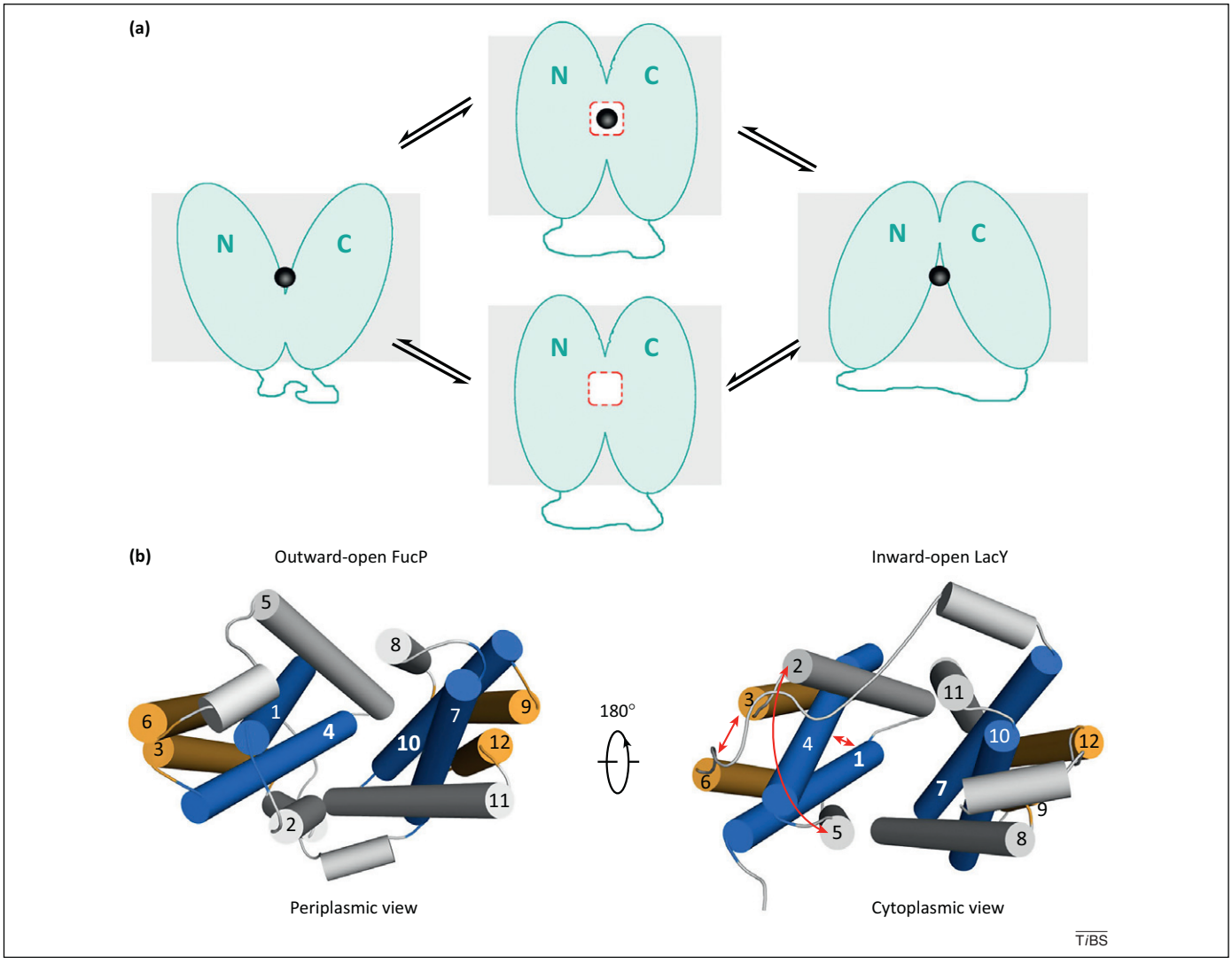

Figure 3. Alternating access of major facilitator superfamily (MFS) transporters. **(a)** Schematic diagram to illustrate the alternating access mechanism for MFS transporters. The substrate is represented by a black sphere, which is bound to a central cavity approximately halfway into the membrane and sandwiched by the discretely folded N and C domains. **(b)** Structural comparison of the outward-open FucP and inward-open LacY suggests major rearrangement in the interdomain contacts during an alternating access cycle. Interestingly, the overall transmembrane segment (TM) organization in the periplasmic view of FucP is similar to that of the cytoplasmic view of LacY except that the positions of the two 3-TM repeats in each domain are swapped. Swapping of the corresponding TMs in the two 3-TM repeats in the N domains of LacY and FucP is indicated by the red double-headed arrows in the right panel.

is never simultaneously exposed to both sides of the membrane. The conformational changes in an active transporter are the molecular basis for the energy coupling between transport of substrate and co-substrate(s).

Structure determination for an MFS transporter in the relevant conformations could potentially validate the alternating access model. Multiple snapshots during the transport cycle of several non-MFS transporters have been captured, including but not limited to the P-type Na^+, K^+-ATPases, the ATP-binding cassette (ABC) maltose transporters, and the LeuT-fold secondary transporters exemplified by LeuT, Mhp1, AdiC, and BetP. Several comprehensive reviews focus on detailed descriptions of these transporters [42–46]. By contrast, obtaining multiple conformations of an MFS protein has proved to be challenging. At present, not a single MFS protein has yielded crystal structures of more than one conformation. Therefore, structural confirmation of the alternating access model has yet to be obtained for any single MFS protein.

The existing MFS structures provide indirect evidence of the alternating access cycle. They represent several distinct conformations during an alternating access cycle, including those of ligand-free and outward-open (FucP), ligand-bound, outward-facing, and partly occluded (XylE), occluded (EmrD), inward-occluded ($PepT_{so}$), and inward-open (LacY, GlpT, and $PepT_{st}$). These conformations appear to reflect different stages of a transport cycle (Figure 1). However, as illustrated by the LeuT-fold transporters, caution must be exercised when using structural comparison of different proteins to make conclusions about conformational changes [46]. Owing to the lack of multiple conformations for any given MFS transporter, visualization of the transport cycle of MFS proteins was derived largely from biochemical and biophysical investigations [4]. Nevertheless, the available structures provide the molecular basis for modeling and molecular dynamics (MD) simulations [38,47,48].

LacY has been a paradigm for the study of alternating access. Prior to structure determination, extensive biochemical examination had already identified key residues for substrate binding and proton translocation [49,50]. A number of LacY structures were obtained, all exhibiting a nearly identical inward-open conformation [28,51–53]. The other conformations of LacY were proposed from multiple biophysical approaches [4]. Several methods showed that substrate binding increases the probability of an outward-open conformation of LacY, including single-molecule fluorescence resonance energy transfer [54], double electron–electron resonance [55], and Trp fluorescence quenching [56]. Structural models of LacY in the outward-open conformation were generated by swapping the inverted 3-TM repeats within each domain as well as FucP-based modeling. These models agree well with biophysical measurements of a potentially outward-open LacY [31,38].

FucP and LacY are two distantly related MFS members that have less than 10% sequence identity. However, the N and C domains of FucP and LacY can be separately superimposed, with RMSD values of 2.86 and 2.90 Å, respectively, indicating highly similar domain structures [31]. Structural comparison of the outward-open FucP and the inward-open LacY reveals interesting features that may reflect shared structural rearrangements of MFS proteins during transport. Owing to the presence of the inverted 3-TM repeats in each domain, the periplasmic view of FucP and the cytoplasmic view of LacY exhibit highly similar structural organization (Figure 3b). By swapping the two repeats in each domain, Radestock and Forrest were able to generate a structural model of LacY in the outward-open conformation [38] that is reminiscent of the one generated using FucP as a template (Figure 3b) [31].

To achieve a LacY-like inward-open conformation, the N and C domains of the outward-open FucP need to undergo concentric rotation of approximately 40° in the opposite directions around an axis parallel to the membrane plane. The outward-to-inward conformational shifts involve considerable rearrangement of the interface between the N and C domains. In the outward-open FucP conformation, the interface between the N and C domains comprises three major contact areas. First, TM4 and TM10 interact with each other at the center of their transmembrane regions, where Glu135 of TM4 and Tyr365 of TM10 form a hydrogen bond [31]. Second, the N-terminal fragment of TM5 is sandwiched by the C-terminal halves of TM8 and TM10. Third, the N-terminal half of TM11 interacts with the C-terminal halves of TM2 and TM4 through mainly hydrophobic interactions. In LacY, the interdomain interactions also involve three areas: contact between TM1 and TM7 at the center, surrounding interactions between the N-terminal half of TM2 and C-terminal half of TM11 on one side, and contacts between the N-terminal half of TM8 and the C-terminal halves of TM1 and TM5 on the other side (Figure 3b). The predicted cycle of conformational changes in LacY involve alternating interactions between TM1 and TM7 and between TM4 and TM10, which are the corresponding TMs in the 3-TM repeats of a MFS fold. Similarly, TM5, TM2, and TM11 also undergo alternating contacts between the outward-open and inward-open conformations. This analysis further corroborates the notion that the 3-TM repeat is the basic structural and functional unit of MFS transporters.

Structural comparison between LacY and FucP appears to support the rocker-switch model that exploits rigid-body rotation of the two domains for alternating access [29,40]. However, MD simulations [57] and site-directed alkylation of a LacY variant containing the single point mutation C154G [58] suggested that local structural rearrangements would occur in addition to domain rotation during a transport cycle. Furthermore, superposition of the inward-occluded $PepT_{so}$ and the inward-open $PepT_{st}$ revealed a major structural divergence in the cytoplasmic halves of TM7, TM10, and TM11, which undergo a hinge motion away from the N domain to open an inner gate [33]. These structural and biophysical observations suggest that the conformational changes in MFS proteins during a transport cycle may be more complex than a simple rocker-switch model to achieve upload and release of the substrate(s) across the membrane.

Substrate binding

Biochemical characterization of LacY [49], GlpT [29], GalP [59], FucP [31,60], $PepT_{st}$ [33], and others identified essential residues for substrate binding. In contrast to the heated controversy about the number and location of substrate-binding sites in LeuT-fold transporters [61], it is generally accepted that MFS proteins contain a single substrate-binding cavity enclosed by the N and C domains and located halfway into the membrane [49]. In LacY, the substrate is mainly coordinated to residues from the N domain, with Glu126 on TM4 and Arg144/Trp151 on TM5 directly involved in galactoside binding [39]. In FucP, residues Glu135 on TM4 and Gln162 on TM5 in the N domain are essential for substrate binding [31]. In $PepT_{st}$, residues Tyr29 and Tyr30 on TM1 and Tyr68 on TM2, all from the N domain, are important for peptide-binding affinity [33]. The first unambiguous picture of substrate coordination by a MFS transporter was recently provided by the structures of XylE in complex with three different ligands: its authentic substrate D-xylose, its inhibitor D-glucose, and a glucose derivative, 6-Br-6-deoxy-D-glucose (6BrGlc), at resolutions of 2.8, 2.9, and 2.6 Å, respectively [34].

The anomalous signal derived from the bromide atom in the 6BrGlc molecule, together with the moderately high resolution, allowed assignment of the bound ligands into the structure of XylE [34]. Unlike LacY, in which the substrate is largely recognized by residues of the N domain [28], the ligand in XylE is mainly coordinated to the C domain (Figure 4a) [34]. Consistent with the biochemical characterization of other MFS transporters, the substrate-binding site of XylE is located halfway into the membrane, at a nearly equal distance between the periplasm and the cytoplasm. TM7, which has a kink in the middle, contributes more than half of the interacting residues for ligand coordination (Figure 4b). The chemically similar D-xylose and D-glucose are recognized by XylE with an almost identical set of interactions [34]. The sugar ring is placed approximately parallel along the cavity-facing side of the C domain. The hydroxyl groups of the ligand are coordinated to polar residues through hydrogen bonds. Similar to many other types of transporters [46], multiple aromatic residues surround the trapped substrate (Figure 4b).

Substrate recognition by predominantly a single domain appears to be a common feature in transporters that are organized into discrete domains. In the primary ABC maltose transporters, the transmembrane domain comprises two subunits, MalF and MalG; maltose is coordinated mainly to MalF [62,63]. In the NAT (nucleobases:ascorbate) family transporter UraA, the substrate uracil is coordinated primarily to residues in the core domain [64]. It remains to be elucidated whether the one-domain coordination of substrate represents a transient state during transport. Such information is particularly important for understanding the coupling mechanism of co-transporters.

The coupling mechanism of MFS proton symporters

MFS proteins include both facilitators and secondary active transporters. Whereas the facilitators catalyze facilitative diffusion of a substrate down its concentration gradient, the secondary active transporters harness the electrochemical potential of ions or solutes to achieve the energetically unfavorable transport of a substrate against its gradient. The MFS active transporters can also be divided into symporters and antiporters, which catalyze the transmembrane movement of two or more substrates in the same or opposite directions, respectively. A full picture of the coupling mechanism is lacking for almost all secondary active transporters.

Among the MFS transporters with known structures, with the exception of the antiporters GlpT and EmrD, all are proton-coupled symporters, which shuttle substrate by exploiting the energy stored in the proton gradient across the membrane. The substrate and proton are co-transported by proton symporters in the same direction at a fixed stoichiometry. Whereas substrate transport requires alternate exposure of the binding site to either side of the membrane, translocation of protons involves protonation and deprotonation of certain residues, most frequently Glu/Asp/His and to a lesser extent Lys/Arg/Tyr. To identify such residues, the effects of point mutation of the candidate residues may be compared in two activities: proton gradient-independent counterflow [65] and proton-coupled active transport. Beginning with LacY, this approach has been successfully applied to a number of transporters.

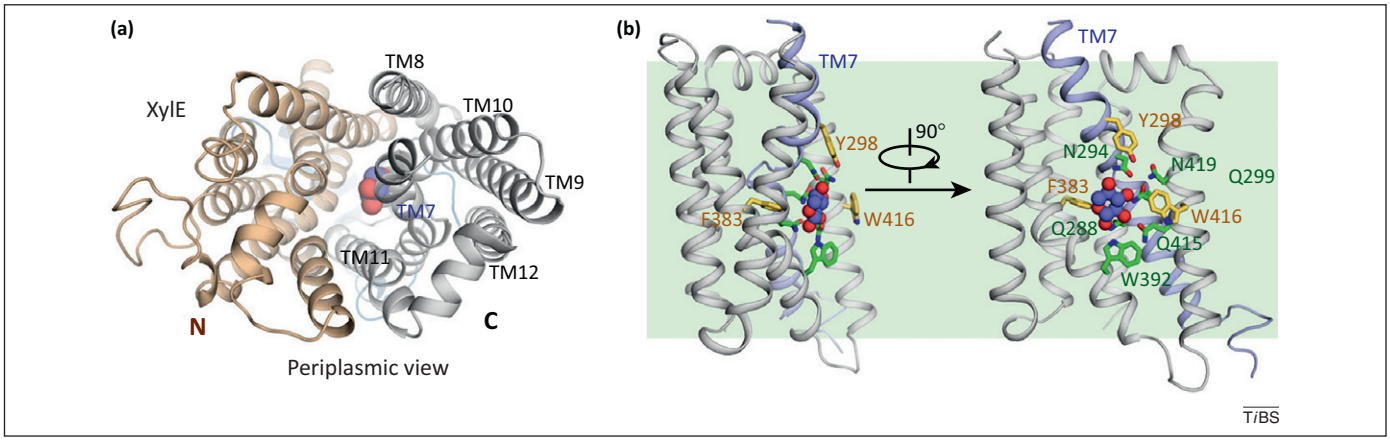

Figure 4. Substrate binding in XylE. **(a)** Periplasmic view of XylE bound to D-xylose. The N and C domains are colored wheat and silver, respectively. D-Xylose is shown as spheres. Note that D-xylose is located closer to the C domain. **(b)** D-Xylose is predominantly coordinated to residues from the C domain of XylE. The coordinating polar and aromatic residues are colored green and yellow, respectively. Transmembrane segment 7 (TM7), which plays a prominent role in substrate binding, is colored lilac.

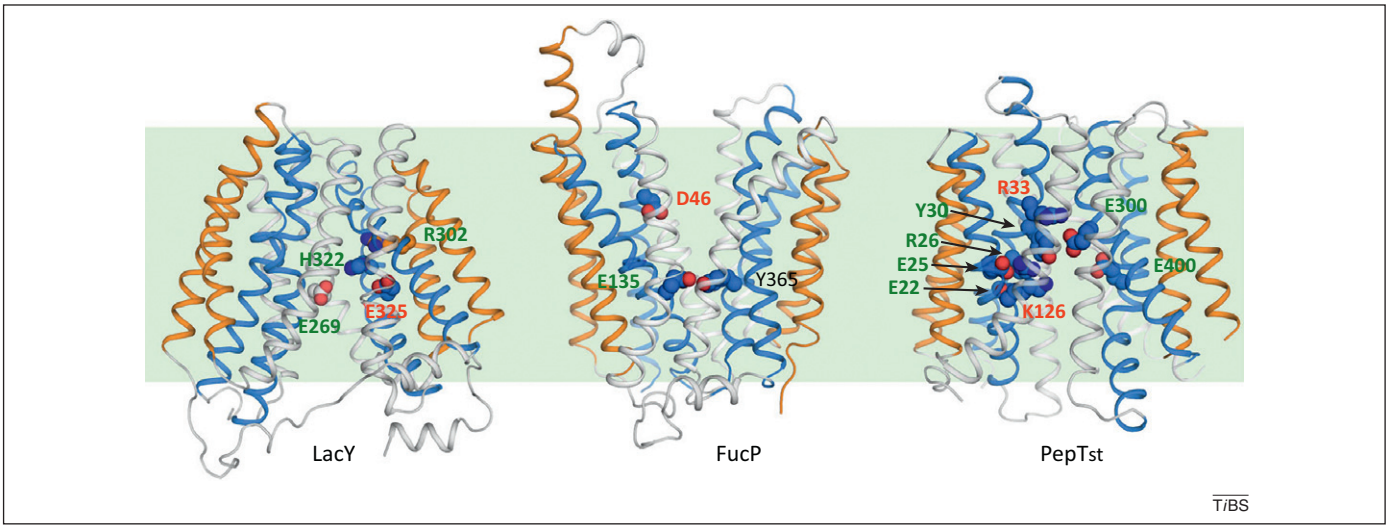

Figure 5. Functionally important residues for proton translocation in the proton symporters LacY, FucP, and $PepT_{st}$. Shown in spheres are the well-characterized residues that are important for proton translocation and coupling. Neutralization of Glu325 in LacY, Asp46 in FucP, and Arg33 and Ly126 in $PepT_{st}$ (all labeled in red) abolished proton-driven active uptake, but retained full activity in counterflow assays.

In LacY, Glu269 on TM8 and His322 on TM10 are indispensable for proton translocation and are important for substrate binding; Glu325 on TM10 is essential for proton release; and Arg302 on TM9 may facilitate deprotonation of Glu325 [47,49]. Notably, all of these residues are located in the C domain. In FucP, Asp46 on TM1 and Glu135 on TM4, both in the N domain, are the primary conserved residues along the transport path that are capable of protonation and deprotonation. Asp46 is irreplaceable for proton coupling but it is not involved in substrate binding; mutation of Glu135 abolished both active transport and counterflow activity of FucP, suggesting its prominent role in substrate binding and transport [31]. The proton-dependent oligopeptide transporter (POT) subfamily, which includes $PepT_{st}$, contains a conserved ExxERFxYY motif that was predicted to be important for both substrate binding and proton translocation. Biochemical characterization of the $_{22}$ExxERFxYY$_{30}$ motif in TM1 of $PepT_{st}$ established the important roles of Glu22, Glu25, Arg26, and Tyr30 in proton translocation, and the role of Tyr29 in peptide specificity. In addition, an adjacent residue, Lys126 from TM4, is essential for proton-driven transport (Figure 5) [33]. It is noteworthy that in all of these transporters, the majority of the key residues for proton translocation are located in TM1, TM4, TM7, and TM10, the first TM in each of the four 3-TM repeats, suggesting functional conservation of MFS proton symporters.

Co-transport of substrate and proton is achieved through conformational changes in the transporter. Therefore, the coupling can be further dissected into three related aspects: coupling between substrate binding/dissociation and conformational changes in the transporter, between substrate binding/dissociation and protonation/deprotonation, and between protonation/deprotonation and conformational shifts in the transporter.

To bind or release substrate, a transporter has to exhibit an open conformation to either side of the lipid bilayer. The correlation between substrate binding and conformational shifts in the transporter has been investigated using multiple biophysical approaches. Examination of LacY, whose default conformation is inward-open, suggested that sugar binding leads to increased probability that the transporter will adopt an outward-open conformation [4]. Trp fluorescence quenching and MD simulation for FucP suggested that L-fucose binding may induce a transition from an outward-open to an occluded conformation [60]. Closure of the N and C domains naturally prevents the escape of bound substrate, as seen in ligand-bound, partly occluded XylE structures [34].

For proton symporters, co-transport of the substrate and the proton(s) is obligatory. Several lines of evidence suggest that protonation may precede substrate binding. Examination of the effect of pH on the apparent substrate-binding affinity of LacY revealed an unexpectedly high pK_a of approximately 10.5, whereas the affinity for sugar binding remained unchanged within the pH range 5.5–9.0. This observation indicates that LacY might be fully protonated prior to sugar binding [66]. A similar conclusion may be made for FucP, for which protonation of Asp46 appears to assist substrate binding, as suggested by MD simulations [31]. However, a recent kinetic study of LacY using D_2O suggested a more complex mechanism in which sugar binding involves internal proton transfer within the transporter [67]. Whereas our understanding of protonation-dependent substrate binding remains rather preliminary, the effect of substrate binding and release on proton translocation is even less characterized because of technical challenges. In FucP, the bound L-fucose may provide a path for proton relay in the form of hydronium from Asp46 to Glu135 [31], a speculation that awaits direct experimental evidence.

Equally perplexing is the interdependence between proton translocation and conformational changes in the protein. A preliminary understanding is mainly derived from MD simulations. In the outward-open structure of FucP, Glu135 onTM7 is hydrogen-bonded to Tyr365 on TM10. MD simulations suggest that this hydrogen bond is stable only if Glu135 is deprotonated. On protonation, the bond is probably broken, which may

trigger a subsequent outward-to-inward conformational switch [31]. Interestingly, domain-based superposition of $PepT_{st}$ and FucP suggested a similar deprotonation-dependent hydrogen bond between Lys126 on TM4 and Glu400 on TM10 in the predicted outward-facing $PepT_{st}$ (Figure 5) [33]. MD simulations of apo-LacY in a phosphatidylethanolamine bilayer showed that deprotonation of Glu325 may result in major structural shifts [47]. Despite the aforementioned progress, the coupling mechanism remains the most puzzling question to address for MFS co-transporters.

Perspective

The advent of new MFS structures has provided additional insights into the common features of the MFS fold and the functional mechanisms of this important transporter family. The pseudosymmetry of the discretely folded N and C domains and the 3+3 inverted repeats within each domain constitute the molecular basis for alternating access and co-transport coupling. Despite these latest advances, much remains to be learned to achieve a comprehensive understanding of the MFS transport proteins.

All available MFS structures are of bacterial proteins. Not a single crystal structure is available for any eukaryotic MFS protein, especially for the physiologically and pathologically significant MFS members. The limited structural information available for eukaryotic MFS transporters was mainly derived from homology modeling, which is insufficient for rational drug design or mechanistic elucidation. Structural determination of eukaryotic proteins represents a major challenge for the structural biology of MFS transporters, and perhaps for all membrane proteins in general.

All MFS structures were obtained by crystallization in detergents. None of the structures was generated in a lipid bilayer. Growing evidence shows that detergents may interfere with the function of membrane receptors, channels, and transporters [68–73]. In the structure of FucP, β-NG occupies the substrate-binding site and competes with L-fucose for binding to FucP [31]. MD simulations of LacY revealed lipid-dependent dynamics [47]. In recent years, application of a lipidic cubic phase (LCP) has greatly assisted crystallization and structural determination of G-protein-coupled receptors (GPCRs) [74]. Crystallization of MFS transporters in bicelle or in meso phase may help to capture different conformations of the transporters discussed above.

Although the structures of different MFS proteins were captured in distinct conformations that together constitute an alternating access cycle, the lack of structural information for a single protein in different conformational states hampers our understanding. Structures of additional conformations for any structurally known MFS protein are in high demand. Techniques such as inclusion of antibody fragments or nanobodies [75,76], chemical crosslinking [18,63,77], and introduction of specific point mutations [78,79] may help to capture additional conformations.

Finally, the central question in our understanding of MFS transporters, and probably for all active transporters in general, is the coupling mechanism. The development and application of novel biochemical, biophysical, and computational approaches may be required to address this important question. For example, Fourier-transform infrared spectroscopic studies revealed water-mediated intraprotein proton transfer for bacteriorhodopsin [80]. Can similar techniques be applied to study proton translocation in the MFS proton symporters? Furthermore, rapid development in the application of X-ray free-electron lasers has provided unprecedented opportunity for femtosecond crystallography, which may be applied to the study of membrane transporters [81,82].

Acknowledgments

This work was supported by funds from the Ministry of Science and Technology (grant numbers 2009CB918802 and 2011CB910501), Projects 31125009 and 91017011 of the National Natural Science Foundation of China, and funds from Tsinghua University. The research of N.Y. was supported in part by an International Early Career Scientist grant from the Howard Hughes Medical Institute.

References

1 Pao, S.S. *et al.* (1998) Major facilitator superfamily. *Microbiol. Mol. Biol. Rev.* 62, 1–34
2 Marger, M.D. and Saier, M.H., Jr (1993) A major superfamily of transmembrane facilitators that catalyse uniport, symport and antiport. *Trends Biochem. Sci.* 18, 13–20
3 Reddy, V.S. *et al.* (2012) The major facilitator superfamily (MFS) revisited. *FEBS J.* 279, 2022–2035
4 Kaback, H.R. *et al.* (2011) The alternating access transport mechanism in LacY. *J. Membr. Biol.* 239, 85–93
5 Guan, L. and Kaback, H.R. (2006) Lessons from lactose permease. *Annu. Rev. Biophys. Biomol. Struct.* 35, 67–91
6 Eldar, A. and Elowitz, M.B. (2010) Functional roles for noise in genetic circuits. *Nature* 467, 167–173
7 Choi, P.J. *et al.* (2008) A stochastic single-molecule event triggers phenotype switching of a bacterial cell. *Science* 322, 442–446
8 Henderson, P.J.F. and Baldwin, S.A. (2012) Structural biology: bundles of insights into sugar transporters. *Nature* 490, 348–350
9 Ozcan, S. and Johnston, M. (1999) Function and regulation of yeast hexose transporters. *Microbiol. Mol. Biol. Rev.* 63, 554–569
10 Buttner, M. (2007) The monosaccharide transporter(-like) gene family in Arabidopsis. *FEBS Lett.* 581, 2318–2324
11 Li, F. *et al.* (2011) Characterization of sucrose transporter alleles and their association with seed yield-related traits in *Brassica napus* L. *BMC Plant Biol.* 11, 168
12 Wilson-O'Brien, A.L. *et al.* (2010) Evolutionary ancestry and novel functions of the mammalian glucose transporter (GLUT) family. *BMC Evol. Biol.* 10, 152
13 Henderson, P.J. and Maiden, M.C. (1990) Homologous sugar transport proteins in *Escherichia coli* and their relatives in both prokaryotes and eukaryotes. *Philos. Trans. R. Soc. Lond. B: Biol. Sci.* 326, 391–410
14 Gbelska, Y. *et al.* (2006) Evolution of gene families: the multidrug resistance transporter genes in five related yeast species. *FEMS Yeast Res.* 6, 345–355
15 Mandal, A. *et al.* (2012) A key structural domain of the *Candida albicans* Mdr1 protein. *Biochem. J.* 445, 313–322
16 Dias, P.J. *et al.* (2010) Evolution of the 12-spanner drug:H+ antiporter DHA1 family in hemiascomycetous yeasts. *OMICS* 14, 701–710
17 Hassan, K.A. *et al.* (2011) Roles of DHA2 family transporters in drug resistance and iron homeostasis in *Acinetobacter* spp. *J. Mol. Microbiol. Biotechnol.* 20, 116–124
18 Fluman, N. *et al.* (2012) Dissection of mechanistic principles of a secondary multidrug efflux protein. *Mol. Cell* 47, 777–787
19 Tirosh, O. *et al.* (2012) Manipulating the drug/proton antiport stoichiometry of the secondary multidrug transporter MdfA. *Proc. Natl. Acad. Sci. U.S.A.* 109, 12473–12478
20 Scheffer, I.E. (2012) GLUT1 deficiency: a glut of epilepsy phenotypes. *Neurology* 78, 524–525
21 Brockmann, K. (2009) The expanding phenotype of GLUT1-deficiency syndrome. *Brain Dev.* 31, 545–552

22 Santer, R. *et al.* (1997) Mutations in *GLUT2*, the gene for the liver-type glucose transporter, in patients with Fanconi–Bickel syndrome. *Nat. Genet.* 17, 324–326
23 Simpson, I.A. *et al.* (2008) The facilitative glucose transporter GLUT3: 20 years of distinction. *Am. J. Physiol.* 295, E242–E253
24 Amann, T. and Hellerbrand, C. (2009) GLUT1 as a therapeutic target in hepatocellular carcinoma. *Expert Opin. Ther. Targets* 13, 1411–1427
25 Mueckler, M. (1993) The molecular biology of glucose transport: relevance to insulin resistance and non-insulin-dependent diabetes mellitus. *J. Diabetes Complications* 7, 130–141
26 Nelson, D.L. and Cox, M.M. (2008) *Lehninger Principles of Biochemistry*, W.H. Freeman
27 Leto, D. and Saltiel, A.R. (2012) Regulation of glucose transport by insulin: traffic control of GLUT4. *Nat. Rev.* 13, 383–396
28 Abramson, J. *et al.* (2003) Structure and mechanism of the lactose permease of *Escherichia coli*. *Science* 301, 610–615
29 Huang, Y. *et al.* (2003) Structure and mechanism of the glycerol-3-phosphate transporter from *Escherichia coli*. *Science* 301, 616–620
30 Yin, Y. *et al.* (2006) Structure of the multidrug transporter EmrD from *Escherichia coli*. *Science* 312, 741–744
31 Dang, S. *et al.* (2010) Structure of a fucose transporter in an outward-open conformation. *Nature* 467, 734–738
32 Newstead, S. *et al.* (2011) Crystal structure of a prokaryotic homologue of the mammalian oligopeptide-proton symporters, PepT1 and PepT2. *EMBO J.* 30, 417–426
33 Solcan, N. *et al.* (2012) Alternating access mechanism in the POT family of oligopeptide transporters. *EMBO J.* 31, 3411–3421
34 Sun, L. *et al.* (2012) Crystal structure of a bacterial homologue of glucose transporters GLUT1-4. *Nature* 490, 361–366
35 Jin, J. *et al.* (2001) Twelve-transmembrane-segment (TMS) version (DeltaTMS VII-VIII) of the 14-TMS Tet(L) antibiotic resistance protein retains monovalent cation transport modes but lacks tetracycline efflux capacity. *J. Bacteriol.* 183, 2667–2671
36 Foster, D.L. *et al.* (1983) Structure of the lac carrier protein of *Escherichia coli*. *J. Biol. Chem.* 258, 31–34
37 Hvorup, R.N. and Saier, M.H., Jr (2002) Sequence similarity between the channel-forming domains of voltage-gated ion channel proteins and the C-terminal domains of secondary carriers of the major facilitator superfamily. *Microbiology* 148, 3760–3762
38 Radestock, S. and Forrest, L.R. (2011) The alternating-access mechanism of MFS transporters arises from inverted-topology repeats. *J. Mol. Biol.* 407, 698–715
39 Zhou, Y. *et al.* (2012) Role of the irreplaceable residues in the LacY alternating access mechanism. *Proc. Natl. Acad. Sci. U.S.A.* 109, 12438–12442
40 Law, C.J. *et al.* (2008) Ins and outs of major facilitator superfamily antiporters. *Annu. Rev. Microbiol.* 62, 289–305
41 Jardetzky, O. (1966) Simple allosteric model for membrane pumps. *Nature* 211, 969–970
42 Palmgren, M.G. and Nissen, P. (2011) P-type ATPases. *Annu. Rev. Biophys.* 40, 243–266
43 Morth, J.P. *et al.* (2011) A structural overview of the plasma membrane Na^+,K^+-ATPase and H^+-ATPase ion pumps. *Nat. Rev.* 12, 60–70
44 Oldham, M.L. *et al.* (2008) Structural insights into ABC transporter mechanism. *Curr. Opin. Struct. Biol.* 18, 726–733
45 Rees, D.C. *et al.* (2009) ABC transporters: the power to change. *Nat. Rev.* 10, 218–227
46 Shi, Y. (2013) Common folds and transport mechanisms of secondary active transporters. *Annu. Rev. Biophys.* http://dx.doi.org/10.1146/annurev-biophys-083012-130429
47 Andersson, M. *et al.* (2012) Proton-coupled dynamics in lactose permease. *Structure* 20, 1893–1904
48 Madej, M.G. *et al.* (2012) Apo-intermediate in the transport cycle of lactose permease (LacY). *Proc. Natl. Acad. Sci. U.S.A.* 109, E2970–E2978
49 Kaback, H.R. *et al.* (2001) The kamikaze approach to membrane transport. *Nat. Rev.* 2, 610–620
50 Smirnova, I. *et al.* (2011) Lactose permease and the alternating access mechanism. *Biochemistry* 50, 9684–9693
51 Guan, L. *et al.* (2007) Structural determination of wild-type lactose permease. *Proc. Natl. Acad. Sci. U.S.A.* 104, 15294–15298
52 Mirza, O. *et al.* (2006) Structural evidence for induced fit and a mechanism for sugar/H^+ symport in LacY. *EMBO J.* 25, 1177–1183
53 Chaptal, V. *et al.* (2011) Crystal structure of lactose permease in complex with an affinity inactivator yields unique insight into sugar recognition. *Proc. Natl. Acad. Sci. U.S.A.* 108, 9361–9366
54 Majumdar, D.S. *et al.* (2007) Single-molecule FRET reveals sugar-induced conformational dynamics in LacY. *Proc. Natl. Acad. Sci. U.S.A.* 104, 12640–12645
55 Smirnova, I. *et al.* (2007) Sugar binding induces an outward facing conformation of LacY. *Proc. Natl. Acad. Sci. U.S.A.* 104, 16504–16509
56 Smirnova, I. *et al.* (2009) Probing of the rates of alternating access in LacY with Trp fluorescence. *Proc. Natl. Acad. Sci. U.S.A.* 106, 21561–21566
57 Jensen, M. *et al.* (2007) Sugar transport across lactose permease probed by steered molecular dynamics. *Biophys. J.* 93, 92–102
58 Nie, Y. *et al.* (2008) The Cys154→Gly mutation in LacY causes constitutive opening of the hydrophilic periplasmic pathway. *J. Mol. Biol.* 379, 695–703
59 Patching, S.G. *et al.* (2008) Relative substrate affinities of wild-type and mutant forms of the *Escherichia coli* sugar transporter GalP determined by solid-state NMR. *Mol. Membr. Biol.* 25, 474–484
60 Sugihara, J. *et al.* (2012) Dynamics of the L-fucose/H^+ symporter revealed by fluorescence spectroscopy. *Proc. Natl. Acad. Sci. U.S.A.* 109, 14847–14851
61 Lim, H-H. and Miller, C. (2012) It takes two to transport, or is it one? *Nat. Struct. Mol. Biol.* 19, 129–130
62 Oldham, M.L. *et al.* (2007) Crystal structure of a catalytic intermediate of the maltose transporter. *Nature* 450, 515–521
63 Oldham, M.L. and Chen, J. (2011) Crystal structure of the maltose transporter in a pretranslocation intermediate state. *Science* 332, 1202–1205
64 Lu, F. *et al.* (2011) Structure and mechanism of the uracil transporter UraA. *Nature* 472, 243–246
65 Xie, H. (2008) Activity assay of membrane transport proteins. *Acta Biochim. Biophys. Sin. (Shanghai)* 40, 269–277
66 Smirnova, I.N. *et al.* (2008) Protonation and sugar binding to LacY. *Proc. Natl. Acad. Sci. U.S.A.* 105, 8896–8901
67 Smirnova, I. *et al.* (2012) Role of protons in sugar binding to LacY. *Proc. Natl. Acad. Sci. U.S.A.* 109, 16835–16840
68 Chung, K.Y. *et al.* (2012) Role of detergents in conformational exchange of a G protein-coupled receptor. *J. Biol. Chem.* 287, 36305–36311
69 Schmidt, D. *et al.* (2009) A gating model for the archeal voltage-dependent K^+ channel KvAP in DPhPC and POPE:POPG decane lipid bilayers. *J. Mol. Biol.* 390, 902–912
70 Stouffer, A.L. *et al.* (2008) Structural basis for the function and inhibition of an influenza virus proton channel. *Nature* 451, 596–599
71 Sharma, M. *et al.* (2010) Insight into the mechanism of the influenza A proton channel from a structure in a lipid bilayer. *Science* 330, 509–512
72 Schnell, J.R. and Chou, J.J. (2008) Structure and mechanism of the M2 proton channel of influenza A virus. *Nature* 451, 591–595
73 Quick, M. *et al.* (2012) Experimental conditions can obscure the second high-affinity site in LeuT. *Nat. Struct. Mol. Biol.* 19, 207–211
74 Caffrey, M. *et al.* (2012) Membrane protein structure determination using crystallography and lipidic mesophases: recent advances and successes. *Biochemistry* 51, 6266–6288
75 Steyaert, J. and Kobilka, B.K. (2011) Nanobody stabilization of G protein-coupled receptor conformational states. *Curr. Opin. Struct. Biol.* 21, 567–572
76 Rasmussen, S.G. *et al.* (2011) Structure of a nanobody-stabilized active state of the β_2 adrenoceptor. *Nature* 469, 175–180
77 Reyes, N. *et al.* (2009) Transport mechanism of a bacterial homologue of glutamate transporters. *Nature* 462, 880–885
78 Gao, X. *et al.* (2010) Mechanism of substrate recognition and transport by an amino acid antiporter. *Nature* 463, 828–832
79 Krishnamurthy, H. and Gouaux, E. (2012) X-Ray structures of LeuT in substrate-free outward-open and apo inward-open states. *Nature* 481, 469–474
80 Garczarek, F. and Gerwert, K. (2006) Functional waters in intraprotein proton transfer monitored by FTIR difference spectroscopy. *Nature* 439, 109–112
81 Boutet, S. *et al.* (2012) High-resolution protein structure determination by serial femtosecond crystallography. *Science* 337, 362–364
82 Schlichting, I. and Miao, J. (2012) Emerging opportunities in structural biology with X-ray free-electron lasers. *Curr. Opin. Struct. Biol.* 22, 613–626